



Variation of biogeochemical cycle of riverine dissolved inorganic carbon and silicon with the cascade damming

Haojun Deng¹ · Zhen Tao¹ · Quanzhou Gao^{1,2,3} · Ling Yao¹ · Yong Feng¹ · Yinhua Li¹ · Jian Ding¹ · Zhengang Wang¹ · Xiaoxi Lyu¹ · Peng Xu¹

Received: 22 February 2020 / Accepted: 4 May 2020 / Published online: 16 May 2020
© Springer-Verlag GmbH Germany, part of Springer Nature 2020

Abstract

To investigate the variation of the biogeochemical cycle of riverine dissolved inorganic carbon (DIC) and silicon (DSi) with the cascade damming, the bicarbonate (HCO_3^-), dissolved silicon (DSi), and other environmental factors within the cascade reservoirs of the lower reaches of Yalongjiang River, passing through the southeastern Qinghai-Tibet Plateau, were systematically analyzed by collecting water samples during the wet season and dry season from 2018 to 2019, respectively. The results showed that the lower ratio of DSi to HCO_3^- (0.044 ± 0.001) was mainly controlled by the domination of carbonate mineral in the sedimentary rock of the Yalongjiang River drainage basin. The DSi: HCO_3^- ratio was positively correlated with discharge ($P < 0.05$), and negatively correlated with the water retention time ($P < 0.01$) and chlorophyll a, implying that the variations of DSi: HCO_3^- ratio were mainly determined by the rock chemical weathering processes and the hydrologic process outside the reservoirs and the biological processes within the cascade reservoirs. The phytoplankton photosynthetic process stoichiometrically assimilated DSi and HCO_3^- , resulted in $3.46 \times 10^4 \text{ t-Si a}^{-1}$ and $1.89 \times 10^4 \text{ t-C a}^{-1}$ sequestering in the cascade reservoirs, respectively. Compared with the situation of dam-free in the lower reaches of Yalongjiang River, the export flux of HCO_3^- and DSi at the mouth of Yalongjiang River was reduced by 11.87% and 62.50%, respectively; the ratio of DSi: HCO_3^- decreased by 36.01% for only building the Ertan dam and 53.15% for the cascade damming, respectively. The water renewal time prolonged from 45 to 126.6 days due to the regulation of the cascade reservoirs in the mainstream. Ultimately, a conceptual model on migration-transformation of DIC and DSi within the cascade reservoirs in the lower reaches of Yalongjiang River was established. These findings demonstrated that riverine cascade damming could extend the biogeochemical coupling cycle of DIC and DSi within the inland aquatic ecosystems and ensure the ecological environment security in the hot-dry valley.

Keywords Bicarbonate · Dissolved silica · Environmental factors · Biogeochemical cycles · Cascade reservoirs

Responsible editor: Philippe Garrigues

✉ Zhen Tao
taozhen@mail.sysu.edu.cn

¹ School of Geography and Planning, Guangdong Key Laboratory for Urbanization and Geosimulation, Sun Yat-sen University, Guangzhou 510275, China

² Southern Laboratory of Ocean Science and Engineering (Guangdong, Zhuhai), Zhuhai 519080, China

³ Key Laboratory of Mineral Resource & Geological Processes of Guangdong Province, Guangzhou 510275, China

Introduction

The export of dissolved and particulate biogenic matter from river to the ocean accounts for 90% of the transportation from land to ocean per year (Tréguer and De La Rocha 2013), maintaining the sustainable development of marine ecosystems. In general, riverine (lacustrine) biogenic matter originated from watershed erosion processes and was changed by the biological processes in the land water. For example, the chemical weathering progress of silicate minerals consumes atmospheric carbon dioxide (CO_2), forming bicarbonate (HCO_3^-), releasing dissolved silica (DSi) and other elements. Partial DSi, dissolved CO_2 , and HCO_3^- are absorbed by phytoplankton (i.e., diatoms) through photosynthesis in rivers, lakes, and reservoirs (Beaulieu et al. 2010; Wang et al. 2016); then, the

dead phytoplankton is decomposed and/or deposited at the bottom of water body (Maavara et al. 2014; Ran et al. 2016). The $\text{DSi}:\text{HCO}_3^-$ ratio is controlled by the weathering process of silicate rock/carbonate rock and the growth/decomposition of phytoplankton (Macuiane et al. 2011; Assmy et al. 2013). The HCO_3^- is the main dissolved inorganic carbon (DIC) species in water (Clark and Fritz 1997) while pH ranging from 8 to 9. Thus, HCO_3^- can be used to represent DIC in the karst catchments (Hélie et al. 2002; Das et al. 2005). Consequently, the $\text{DSi}:\text{HCO}_3^-$ ratio can be used as a tracer for the biogeochemical coupling cycle of DIC and Si in the water body (Wang et al. 2013, 2016; Li et al. 2018). The biogeochemical cycle of terrestrial carbon (C) sequestration was coupled with that of silicon (Si) through mechanisms such as silicate weathering (Taylor et al. 2016) and phytolith C sequestration (Parr and Sullivan 2011; Song et al. 2017). The amount of Si fixed by marine diatom ($240 \times 10^{12} \text{ mol a}^{-1}$) was much higher than that by terrestrial plants ($60 \times 10^{12} \sim 180 \times 10^{12} \text{ mol a}^{-1}$) (Conley 2002; Tréguer and De La Rocha 2013). Hence, the role of phytoplankton in the global coupling cycle of C and Si cannot be ignored. Nitrogen and phosphorus are essential nutritive elements to the growth of autochthonous organisms, and the ratio of N:P may indicate the status of nutritional restrictions and affect the composition of the aquatic communities (Guildford and Hecky 2000; Schindler et al. 2008).

More and more riverine dams have been constructed with increasing human interventions on the earth's surface. By the end of 2018, 59,071 dams higher than 15 m have been constructed on the Earth, 23,841 of which were located in China (<http://www.icold-cigb.org/>). With increasing riverine dam construction, the continuity of the river was interrupted, the hydrologic regime was changed, stratification of heat and nutrients was developed in the inundated river channels, the composition and structure of the aquatic organism, especially algal communities, were altered (Wu et al. 2009; Ran et al. 2013; Castello and Macedo 2016; Winemiller et al. 2016). Consequently, the exported fluxes of freshwater, sediments, nutrients to estuaries, deltas, and coastal ecosystems were changed (Syvitski et al. 2005; Carey and Fulweiler 2012; Hughes et al. 2012; Lu et al. 2016), causing a series of ecological and environment issues (i.e., the decline in the inshore aquaculture industry and the change of coral shell) (Meybeck 1987). Up to date, however, the change of coupling cycle of C and Si caused by cascade damming has not been well reported. Biogenic elements Si and C are assimilated in characteristic stoichiometric ratios by photosynthesis processes of phytoplankton and form biological organism. The Si and C cycles are linked by the biological process in river-reservoir systems. Thus, the stoichiometry ratio of DSi to HCO_3^- could be served as a tracer for the biogeochemical cycles of Si and C in river-reservoir systems (Wang et al. 2013). Therefore, DSi , HCO_3^- , and related water environmental factors (total dissolved solids, sodium, total nitrogen, total phosphorus, and chlorophyll a) were analyzed on the

basis of seasonal sampling in the lower reaches of the Yalongjiang River (LYLJR) to explore the change of biogeochemical coupling cycles of C and Si with cascade damming.

Material and methods

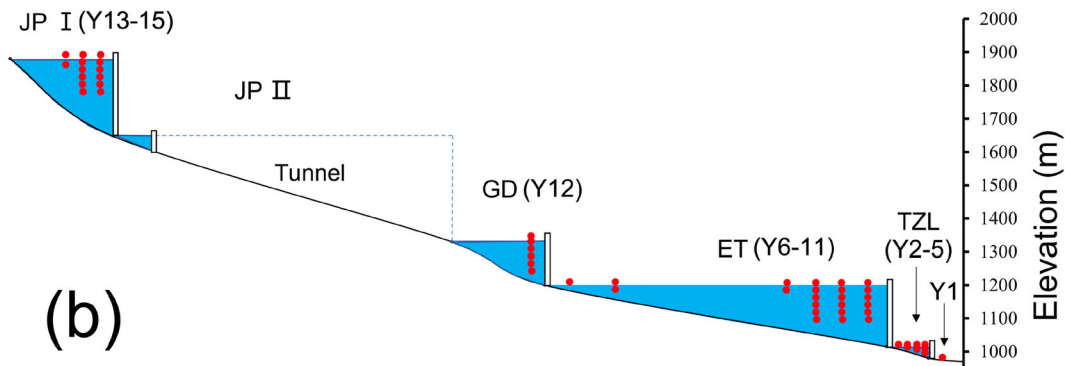
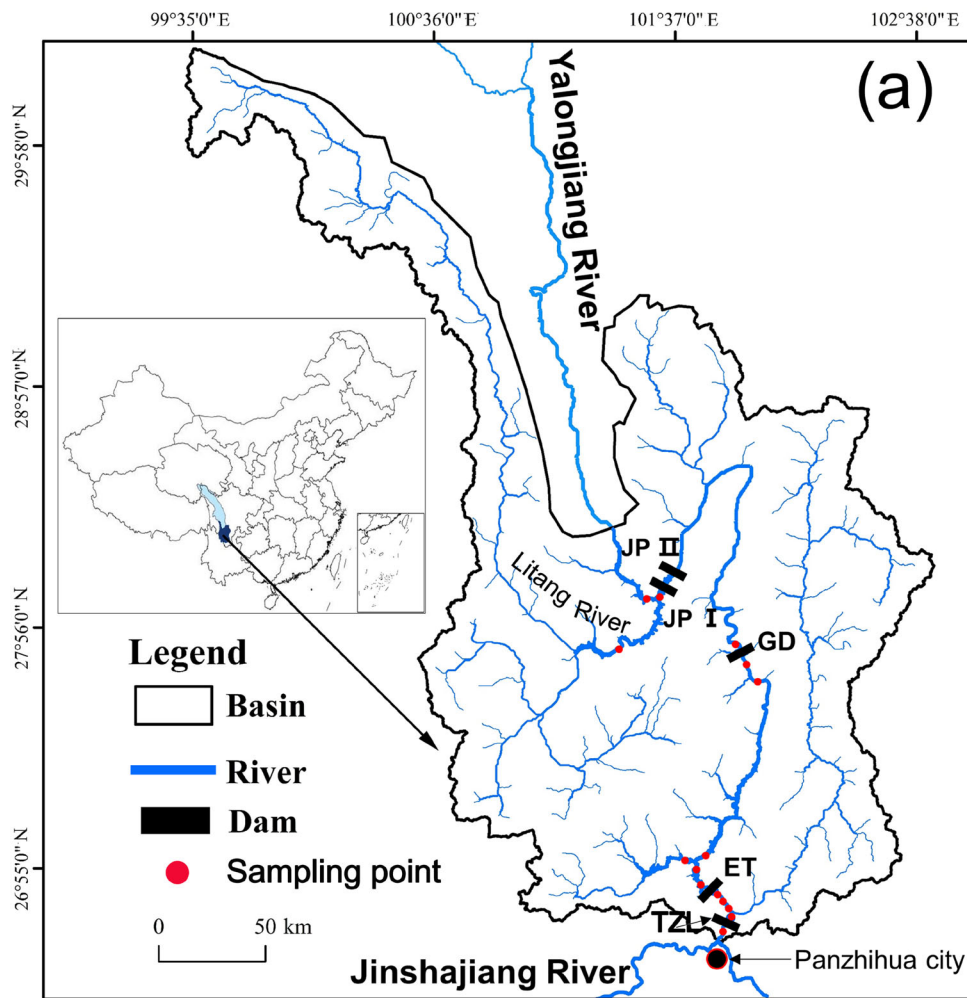
Study area

The Yalongjiang River ($26^\circ 32' \sim 33^\circ 58' \text{ N}$ and $96^\circ 52' \sim 102^\circ 48' \text{ E}$), passing through the southeastern Qinghai-Tibet Plateau, is one of the main tributaries of the Yangtze River (Fig. 1). The total length of the Yalongjiang River is 1571 km with about 3830 m of total drop and $13.6 \times 10^4 \text{ km}^2$ of the total area. The average annual discharge accounts for 13.3% of the total water discharge in the upper reaches of the Yangtze River (He et al. 2015). The Yalongjiang River is divided by upper reaches above Nituo, middle reaches of Nituo to Litang river mouth, lower reaches of Litang river mouth to the Yalongjiang River mouth. The reservoirs of Jinping I (JP I), Jinping II (JP II), Guandi (GD), Ertan (ET), and Tongzilin (TZL) are constructed in the lower reaches of the Yalongjiang River (LYLJR), respectively. The basic information for each reservoir was shown in Fig. 1.

The LYLJR is widely distributed by clastic rocks and carbonate rocks with scattered magmatic rocks and metamorphic rocks (Li et al. 2014). The mean monthly temperature ranges from 6 to 19 °C. The average annual precipitation is approximately 957 mm, of which 93% occurs in the wet season (from May to October), some 7% of total annual precipitation presents in the dry season (from November to April) (Fig. 2) (data from <http://www.cma.gov.cn/>). Consequently, the runoff in the wet season occupies 80.56% of the total annual discharge because of the runoff being mainly fed by atmospheric precipitation (He et al. 2015). In different situations, the average annual discharge at the mouth of the YLJR was $59.26 \times 10^8 \text{ m}^3$ (in the condition of dam-free), $60.13 \times 10^8 \text{ m}^3$ (only ET dam) and $56.90 \times 10^8 \text{ m}^3$ (cascade damming), respectively (Fig. 2b) (data from <http://www.cjw.gov.cn/>). There are natural forests (including mixed woodland, *Leucaena leucocephala* woodland, coniferous and broad-leaved mixed forest land, *Pinus yunnanensis* woodland, etc.), plantations (mango orchard and apple orchard), grassland, and cultivated land in the study area (Editorial Committee for Vegetation Map of China 2001).

Sampling and measurements

On the basis of the seasonal variation of the reservoirs regulation, 15 profiles were selected in the reservoirs (Fig. 1). Samples were taken from downstream of the TZL dam to the tail of the JP I reservoir. A total of 156 water samples were collected at 0.5, 5, 10, 15, 20, and 25 m depth at the sites of ET



365	358	178	33	15	Distance from estuary (m)
77.6	0.14	7.53	58	0.72	Total storage capacity (10^8 m^3)
1880	1646	1330	1200	1015	Normal water level (m)
1220	1220	1430	1670	1920	Annual water discharge (m^3/s)
2014	2014	2013	1998	2015	Completion time (a)
75	0.1	6	45	0.5	Retention time (day)
305	37	168	240	67	Height of dams (m)
59.2	7.5	58	145	18	Backwater length (km)

Fig. 1 a The sketch of sampling sites in the LYLJR basin (data from <http://www.gscloud.cn/>). b Basic information of the cascade reservoirs (data from <http://www.ylhdc.com.cn/>)

(Y6-Y8), GD (Y12), and JP I (Y13-Y14); 0.5, 5, and 10 m depth at the sites of Y2; and 0.5 and 5 m depth at the sites of Y3, Y4, Y9, Y10, and Y15, as well as surface water (0.5 m) at the sites of Y1, Y5, and Y11, in January (dry season) and July (wet season) from 2018 to 2019, respectively. Water samples in the JP II reservoir failed to collect because of the majority of the reservoir covered by tunnels.

Water temperature (T), pH, total dissolved solid (TDS), and chlorophyll a (Chl a) were measured in situ. T, pH, and TDS were measured by Ultrameter™ Model 6P with the precision of ±0.10 °C, ±0.20, and ±0.10 mg L⁻¹, respectively. The concentrations of Chl a were measured by the Hydrolab DS5 (Hach Corporation, USA, the test precision is ±0.01 µg L⁻¹).

The water samples were kept refrigerated at 4 °C before measurements, a portion of each sample was filtrated through

a filter membrane of 0.45 µm, and then analyzed for ion concentrations. Samples for cations were acidified to pH < 2 with HNO₃. The concentrations of DSi and sodium (Na⁺) were analyzed by the inductively coupled plasma atomic emission (ICP-AES) and analytical precision was better than 0.5%. The HCO₃⁻ was titrated by the automatic titration equipment TitraLab TIM856 (Hach Corporation, USA), with three times repeated analysis, analytical precisions in this study were better than 0.05 mL. The pH values of water samples ranged from 7.94 to 9.12 with an average of 8.39; the concentration of HCO₃⁻ was approximately equal to the total alkalinity (Hélie et al. 2002; Li et al. 2018). The total nitrogen (TN) and total phosphorus (TP) were analyzed according to the standard colorimetric methods (APHA 2005) and the analytical precision was better than 2%.

The hydrologic data were from the Changjiang Hydrological Committee (<http://www.cjw.gov.cn/>).

Calculation of the primary production of the diatom

In the terrestrial freshwater ecosystem, diatom always contributes to most of the primary production (Wang et al. 2016). Hence, DSi assimilated by diatoms may be served as the DSi absorbed by algae. On the basis of Chl a concentration and other indicators in the reservoir, the primary production of the diatom and the anabolic HCO₃⁻ by diatom in the reservoir can be estimated (Ran et al. 2016). Cadée and Hegeman (1974) calculated the anabolic organic carbon by diatom:

$$P_c = P_s \times Z \times t/2 \tag{1}$$

where P_c is the carbon fixation (mg·C·m⁻² day⁻¹) in the euphotic zone; P_s is the potential primary production (mg·C·m⁻³ h⁻¹). Z is the euphotic depth (m); t is the daily exposure time (h day⁻¹).

The potential primary production (P_s) was calculated as follows:

$$P_s = Chl\ a \times q \tag{2}$$

where the $Chl\ a$ is the Chl a concentration (mg m⁻³); the q is the assimilation factor ($q = 1.13\ mg\cdot C\cdot mg\cdot Chl\ a^{-1}\ h^{-1}$, Behrenfeld and Falkowski 1997).

The euphotic depth (Z) was calculated as follows:

$$Z = 4.605/K_d \tag{3}$$

where, K_d is the diffuse attenuation coefficient (m⁻¹)(Fang et al. 2010). According to formula (3), the euphotic depth (Z) of the JP I, GD, ET, and TZL was 4.66 m, 7.06 m, 11.63 m, and 8.27 m, respectively.

In terms of the daily exposure time of Panzhihua and Xichang (<http://tjj.sc.gov.cn/>), the t of TZL and ET reservoirs is 7.85 (h day⁻¹), and that of GD and JP I reservoirs is 7.25 (h day⁻¹).

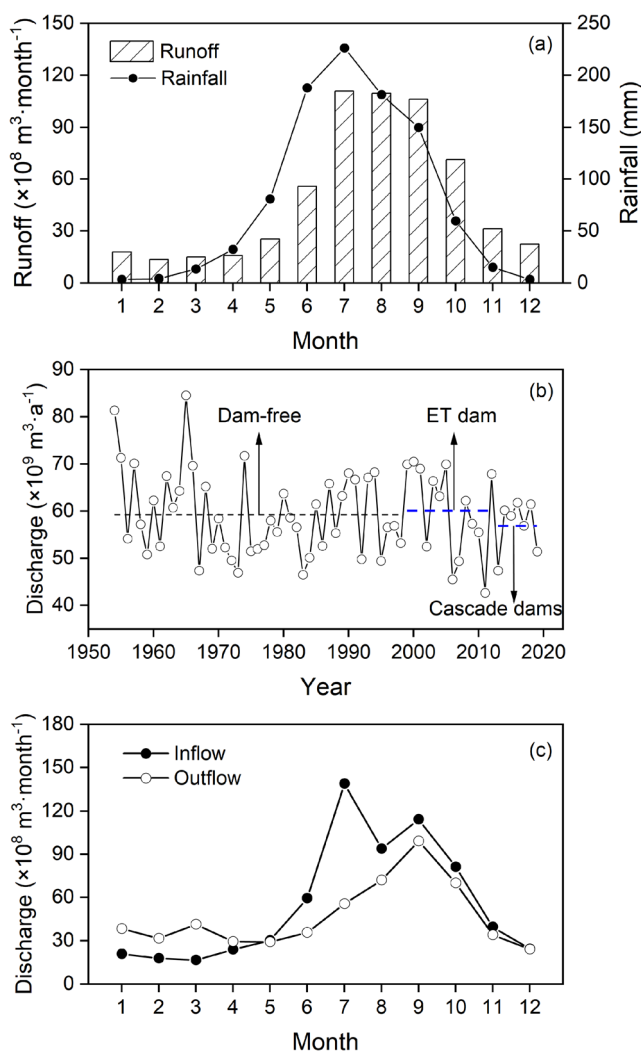


Fig. 2 a Monthly mean rainfall and runoff over the years in the LYLJR (rainfall data from <http://www.cma.gov.cn/runoffdata> from: <http://www.cjw.gov.cn/>). b Discharge variation at the mouth of the Yalongjiang River (<http://www.cjw.gov.cn/>). c Monthly variation of inflow and outflow of the Yalongjiang cascade reservoirs in the sampling years (<http://www.cjw.gov.cn/>)

The Si absorbed by diatoms (P_{Si} , mg·Si·m⁻² day⁻¹) can be calculated (Brzezinski 1985):

$$P_{Si} = 28 \times (\text{Si}/C) \times P_c/12 \quad (4)$$

where Si/C is the stoichiometric ratio of freshwater diatoms (0.79) (Sicko-Goad et al. 1984).

Export flux calculation and its calibration

For the Yalongjiang River basin, the export flux (F_{load}) of DSi and HCO₃⁻ was calculated respectively on the basis of the empirical formulas (5):

$$F_{\text{load}} = C \times Q \quad (5)$$

where F_{load} was the flux of HCO₃⁻ and DSi ($\times 10^6$ t a⁻¹), respectively, C was the concentration of HCO₃⁻ and DSi (mg L⁻¹) respectively, and Q was the discharge ($\times 10^8$ m³ a⁻¹).

The relative errors (δ) for the fluxes was calculated as follows:

$$\delta = \left(\sum_{i=1}^n \left| \frac{Q_i C_i}{n Q_a C_a} - 1 \right| \right) \times 100\% \quad (6)$$

where n is the number of samples in 1 year, Q_i was monthly discharge, Q_a was annual average discharge, C_i was the concentration of HCO₃⁻ and DSi, and C_a was HCO₃⁻ and DSi annual average value (Ran et al. 2016).

Statistical analysis

The two-tailed t test was employed to identify the difference of selected variables between the dry season and the wet season. Simple linear regression analysis was conducted to coordinate the correlations between the DSi:HCO₃⁻ ratio and environmental factors, water retention time and discharge, respectively. Stepwise regression analysis was used to eliminate the collinearity of the independent variables (Kolasa-Wiecek 2015). One-way ANOVA in conjunction with Duncan test was used to uncover the change of the DSi:HCO₃⁻ ratio in different situations (including (1) dam-free on the river, (2) the Ertan dam being built only (ET dam), and (3) the cascade dams being built (cascade dams)) in the mainstream of the LYLJR, respectively. Statistical significance in this study was specified at $P < 0.05$.

Results

Spatio-temporal variation

The HCO₃⁻ was the main anion in the LYLJR. The HCO₃⁻ concentration ranged from 1491.08 to 2492.58 $\mu\text{mol L}^{-1}$ with

an average of $2147.53 \pm 18.17 \mu\text{mol L}^{-1}$ in the study area (Fig. 3a). The DSi concentration varied from 38.39 to 130.89 $\mu\text{mol L}^{-1}$ with an average of $92.23 \pm 1.75 \mu\text{mol L}^{-1}$ (Fig. 3b). Concentrations of DSi were significantly higher in the wet season ($105.31 \pm 16.95 \mu\text{mol L}^{-1}$) than that ($75.18 \pm 1.65 \mu\text{mol L}^{-1}$) in the dry season. However, the concentrations of HCO₃⁻ were remarkably higher in the dry season ($2286.28 \pm 11.60 \mu\text{mol L}^{-1}$) than that ($2041.04 \pm 25.50 \mu\text{mol L}^{-1}$) in the wet season ($P < 0.05$).

The Chl a and pH in the wet season were higher than those in the dry season (Fig. 3c, d), and the Chl a concentration in the reservoir of JP I, GD, ET, and TZL was different, followed by 5.29 $\mu\text{g L}^{-1}$, 3.77 $\mu\text{g L}^{-1}$, 4.03 $\mu\text{g L}^{-1}$, and 1.26 $\mu\text{g L}^{-1}$, respectively. The Chl a concentration in the JP I reservoir was highest, ET reservoir took second place (Fig. 3c). Mean TDS ($159.10 \pm 1.43 \text{ mg L}^{-1}$) was higher than that (100 mg L^{-1}) of the global river (Gaillardet et al. 1999). The concentration of TDS was higher in the dry season than that in the wet season (Fig. 3e), corresponding to the previous report (Li et al. 2014). The Na⁺ concentration ranged from 140.54 to 245.22 $\mu\text{mol L}^{-1}$ with higher seasonal difference (Fig. 3f). The concentrations of TN in the dry season were higher than that in the wet season (Fig. 3g). However, the concentrations of TP in the wet season were higher by 117.57% than that in the dry season (Fig. 3h).

The DSi:HCO₃⁻ ratio ranged from 0.022 to 0.073 with an average value of 0.044 ± 0.001 in the LYLJR. The different ratio of the DSi:HCO₃⁻ occurred among the reservoir of JP I, GD, ET, and TZL, followed by 0.033, 0.047, 0.044, and 0.047, respectively, and the lower values occurred in the reservoirs of JP I and ET, the higher values were in the released water (Y11, Y5, and Y1, Fig. 3i). The DSi:HCO₃⁻ ratio presented markedly seasonal difference and increased from upstream reservoir (JP I) to downstream reservoir (TZL). The TN:TP in the dry season (63.40 ± 4.10) was significantly higher than that in the wet season (35.75 ± 2.53) (Fig. 3j).

Stratification

The ET and JP I reservoirs showed obvious thermal stratification in the wet season, and the thermocline appeared at the depth of 5–20 m in the water column (Fig. 4). No thermal stratification occurred in the dry season. The highest concentration of Chl a generally appeared at the depth of 5 m and then decreased gradually with increasing water depths. The DSi:HCO₃⁻ ratio changed dramatically in the wet season and varied slightly in the dry season. The averaged ratio of DSi:HCO₃⁻ in the surface layer were lower than that in the depth of 25 m during the period of the wet season in the ET and JP I reservoirs, respectively.

Major environmental factors influencing DSi: HCO₃⁻ stoichiometries

The stepwise regression analysis was carried out to identify the major factors affecting the ratio of DSi:HCO₃⁻ in the study area. Environmental factors (TDS, Chl a, pH, TN, TP, TN:TP, water retention time (WRT), and discharge(D)) were selected to predict the variations of the DSi:HCO₃⁻ ratio.

The quantitative relation between the DSi:HCO₃⁻ ratio (*R*) and the most significant environmental factors was expressed as follows:

$$R_{\text{wet}} = 0.037 - 0.101\text{WRT} + 9.06 \times 10^{-6}D + 0.002\text{TP} \quad (7)$$

$(N = 86, R^2 = 0.574, P < 0.001)$

$$R_{\text{dry}} = 0.422 + 1.804 \times 10^{-4}\text{TDS} - 0.051\text{pH} + 0.001\text{Chla} \quad (8)$$

$(N = 66, R^2 = 0.558, P < 0.001)$

where *R_{dry}* and *R_{wet}* was the DSi:HCO₃⁻ ratio in the dry season and the wet season, respectively. WRT was water retention time (a), and *D* was discharge (m³ s⁻¹). The DSi:HCO₃⁻ ratio was controlled by water retention time, discharge, and TP in the wet season. In the dry season, the DSi:HCO₃⁻ ratio was greatly influenced by TDS, pH, and Chl a concentration.

Primary production in the cascade reservoirs

On the basis of formulas (1) and (4), the primary production of the euphotic zone in the cascade reservoirs ranged from 6.05 to 820.33 mg·C·m⁻² day⁻¹ with an average of (182.91 ± 52.51) mg·C·m⁻² day⁻¹, which was some eight times higher than that in the released water ((23.18 ± 8.26) mg·C·m⁻² day⁻¹). Furthermore, the primary production was different in the JP I, GD, ET, and TZL reservoir, followed by (200.90 ± 41.13) mg·C·m⁻² day⁻¹, (121.02 ± 39.16) mg·C·m⁻² day⁻¹, (344.51 ± 81.60) mg·C·m⁻² day⁻¹, and (65.22 ± 25.89) mg·C·m⁻² day⁻¹, respectively. The diatom primary production ranged from 11.04 to 1498.74 mg·Si·m⁻² day⁻¹ with an average of (387.20 ± 60.06) mg·Si·m⁻² day⁻¹ in the cascade reservoirs, which was about five times higher than that (79.38 ± 21.74) mg·Si·m⁻² day⁻¹ in the released water. And that, the diatom primary production existed difference among the JP I, GD, ET, and TZL reservoir, followed by (367.04 ± 75.15) mg·Si·m⁻² day⁻¹, (221.10 ± 71.55) mg·Si·m⁻² day⁻¹, (629.43 ± 149.08) mg·Si·m⁻² day⁻¹, and (119.15 ± 47.30) mg·Si·m⁻² day⁻¹, respectively.

Obviously, the primary production in the LYLJR was much higher than that (1.8 mg·C·m⁻² day⁻¹) in the mainstream of the Changjiang River (Ran et al. 2016).

Discussion

Response of the DSi: HCO₃⁻ ratio to rock characteristics in the basin

In general, the riverine hydrochemical components are primarily controlled by the natural processes (e.g., tectonic activity, chemical weathering, biological processes, and hydrological processes) and human activities (Olds et al. 2011; Hughes et al. 2012; Mosley et al. 2012; Li et al. 2018), of which rock weathering is the main source of riverine chemical constituent. For example, 79.8% of the TDS was sourced from the carbonate weathering, 16% of the TDS was from the silicate weathering, and 1.4% was from evaporite weathering in the Yalongjiang River (Chen et al. 2002). Riverine DSi is merely from silicate weathering; however, HCO₃⁻ is mainly derived from weathering of silicate and carbonate, and the chemical weathering rate of carbonate rock is 17 times higher than that of silicate rock (Amiotte Suchet and Probst 1993), together with carbonate rock being widely distributed in the LYLJR. The HCO₃⁻ was the main anion in the LYLJR. The concentration of HCO₃⁻ (2147.53 ± 18.17 μmol L⁻¹) was approximately 23 times higher than that of DSi (92.23 ± 1.75 μmol L⁻¹) in the LYLJR. And that, the HCO₃⁻ concentration was higher than that (1991.93 μmol·L⁻¹) of the global rivers (Gaillardet et al. 1999) and that (1732.05 μmol L⁻¹) of the global lakes and reservoirs (Peng et al. 2014; Zhang et al. 2016b; Cui et al. 2017; Li et al. 2017). However, the DSi concentration was lower than that (133.02 μmol L⁻¹) of the global rivers (Gaillardet et al. 1999) and that (122.13 μmol L⁻¹) of the global lakes and reservoirs (Peng et al. 2014; Zhang et al. 2016b; Cui et al. 2017; Li et al. 2017).

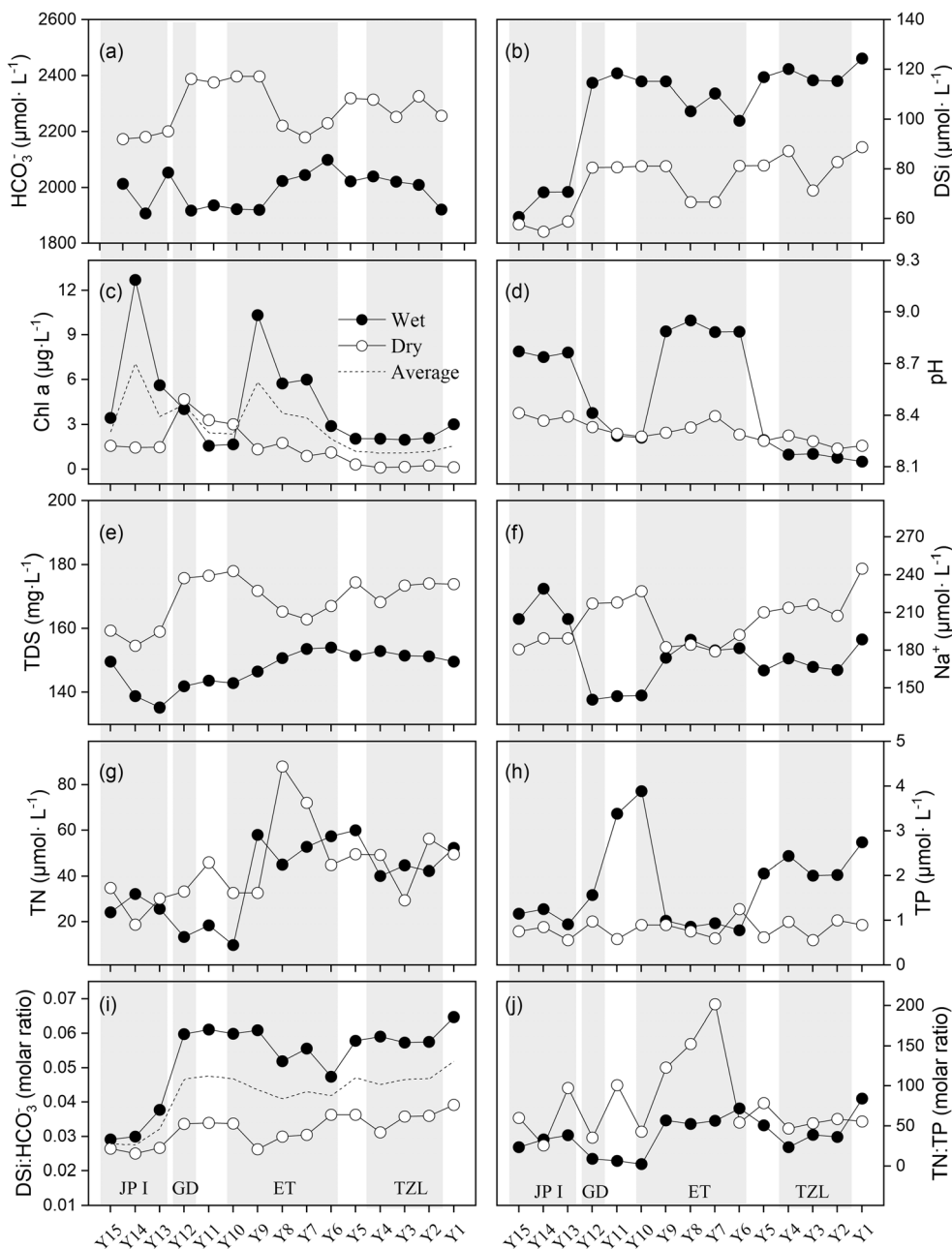
For calcite, one of the main carbonate minerals, the ratio of DSi to HCO₃⁻ is 0, and for a silicate mineral plagioclase, this ratio is 0.67 (Beaulieu et al. 2010). The ratio of DSi to HCO₃⁻ varies from 0 to 0.67 for the river flows through carbonate and/or silicate region (Wang et al. 2016). The averaged ratio of DSi:HCO₃⁻ (0.044 ± 0.001) in the LYLJR was lower, close to that (0.052) of the mainstream of the Yangtze River (Zhang et al. 2016a) and lower than that (0.14) of the global rivers (Gaillardet et al. 1999).

As was noted above, the lower ratio of DSi to HCO₃⁻ was mainly influenced by the dominated carbonate mineral in the sedimentary rock composition of the LYLJR drainage basin.

Change of the relationship between DSi and HCO₃⁻ by cascade damming

A heterotrophic riverine ecosystem may be transformed into an autotrophic “impound river (referred to as reservoir)” by

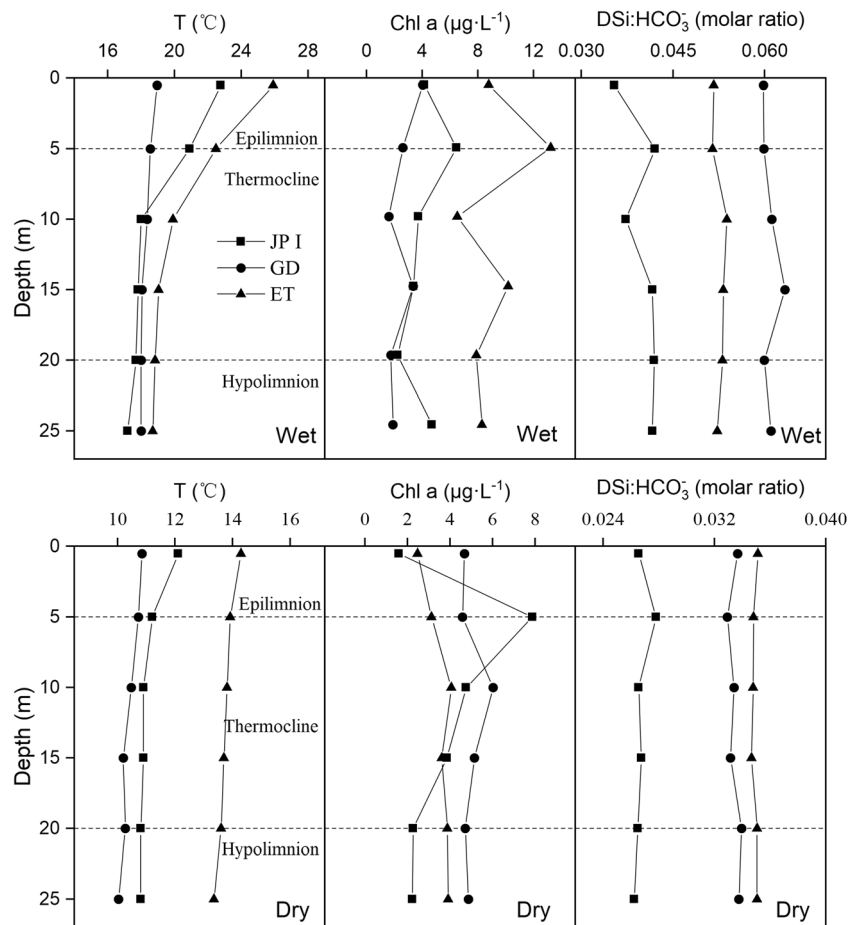
Fig. 3 Variation of the $\text{DSi}:\text{HCO}_3^-$ ratio, the TN:TP ratio and environmental factors in the reservoir surface water of the LYLJR



damming. The changed hydrological regime is in favor of the growth of aquatic organisms. Phytoplankton is one of the major primary producers in lakes and reservoirs. Alga assimilates nutrient elements from their habitats in characteristic stoichiometric ratios (Sterner and Elser 2002). For example, diatoms, one of the most important phytoplankton assemblages in rivers, absorb DSi and form their cell wall. The average ratio of Si to C is 0.79 for freshwater diatoms (Sicko-Goad et al. 1984) and 0.13 for marine diatoms (Brzezinski 1985). The relationship between DSi and HCO_3^- could be altered by diatom stoichiometrically assimilating DSi and dissolved $\text{CO}_2/\text{HCO}_3^-$. The

dissolved CO_2 in these reservoirs mainly results from the conversion of HCO_3^- because the partial pressure of CO_2 in reservoirs is much higher than that of the atmosphere (Wen et al. 2017). The photosynthesis processes of phytoplankton resulted in DSi significantly positively correlating with HCO_3^- ($P < 0.01$) in the studied reservoirs (Fig. 5a), which was consistent with the report in the Wujiang River with cascade dams (Wang et al. 2013). Hence, the cascade damming dramatically changed the negative correlation between DSi and HCO_3^- that was controlled by geological conditions (Gaillardet et al. 1999; Gao et al. 2009; Wang et al. 2013; Zhang et al. 2016b).

Fig. 4 Variations of T, Chl a, and DSi:HCO₃⁻ with depths



Relationship between the DSi: HCO₃⁻ ratio and environmental factors

The relationship between the DSi:HCO₃⁻ ratio and environmental factors in the cascade reservoirs see Fig. 5. The DSi:HCO₃⁻ ratio was significantly negatively correlated with the Chl a in the wet season and pH (*P* < 0.05) (Fig. 5b, c), which was closed to that in the Wujiang River Basin (Wang et al. 2013). This phenomenon was explained by the phytoplankton preferentially absorbing dissolved CO₂ and HCO₃⁻ in the course of photosynthesis, which changed the carbonate balance system in water and caused increasing pH in the euphotic layer (Wang et al. 2015).

Generally, the concentrations of riverine N and P constrain the growth of autotrophic organisms (Yan et al. 2016). The ratio of TN:TP is usually used to judging the restricted nutrients in lakes and marine ecosystems. The TN:TP ratio is less than 20 in the N-deficient ecosystem and greater than 50 in the P-deficient ecosystem (Guildford and Hecky 2000). Pollution from agriculture, domestic and industrial sewage, and water retention time could change the ratio of TN:TP in rivers (Guildford and Hecky 2000; Triplett et al. 2012; Powers et al. 2015; Yan et al. 2016). In the dry season, the ratios of

TN:TP in the study area were greater than 50, indicating that P was the main restricted element in the LYLJR (Fig. 3j). In the wet season, however, the averaged TN:TP ratio was 35.75 resulted from the coupling effect of increasing rainfall and enhancing fertilization owing to vigorous crop growth surrounding the reservoirs (Wu et al. 2010; Jiu et al. 2018). The higher TN and TP in the rainwater runoff were carried into the reservoir and alleviated the limitation of P, which stimulated the biological processes and enhanced the concentrations of Chl a (Fig. 3c, j). The ratios of DSi:HCO₃⁻ were significantly positively correlated with TP (Fig. 5d), implying that DSi, HCO₃⁻, and TP resulted from runoff erosional processes and were changed by algal growth in the LYLJR. The positive correlation between the ratios of DSi:HCO₃⁻ and TP was consistent with that in the Lower Lakes of Australia during the post-drought period (Li et al. 2018) but inconsistent with that in the Wujiang River (Wang et al. 2013). Obviously, the relationship between the DSi:HCO₃⁻ ratios and TP was uncertainty.

In this study, we found that the DSi:HCO₃⁻ ratio was significantly positively correlated with the discharge (Fig. 5e). This phenomenon can be explained by the DSi and HCO₃⁻ mainly resulted from chemical weathering processes and

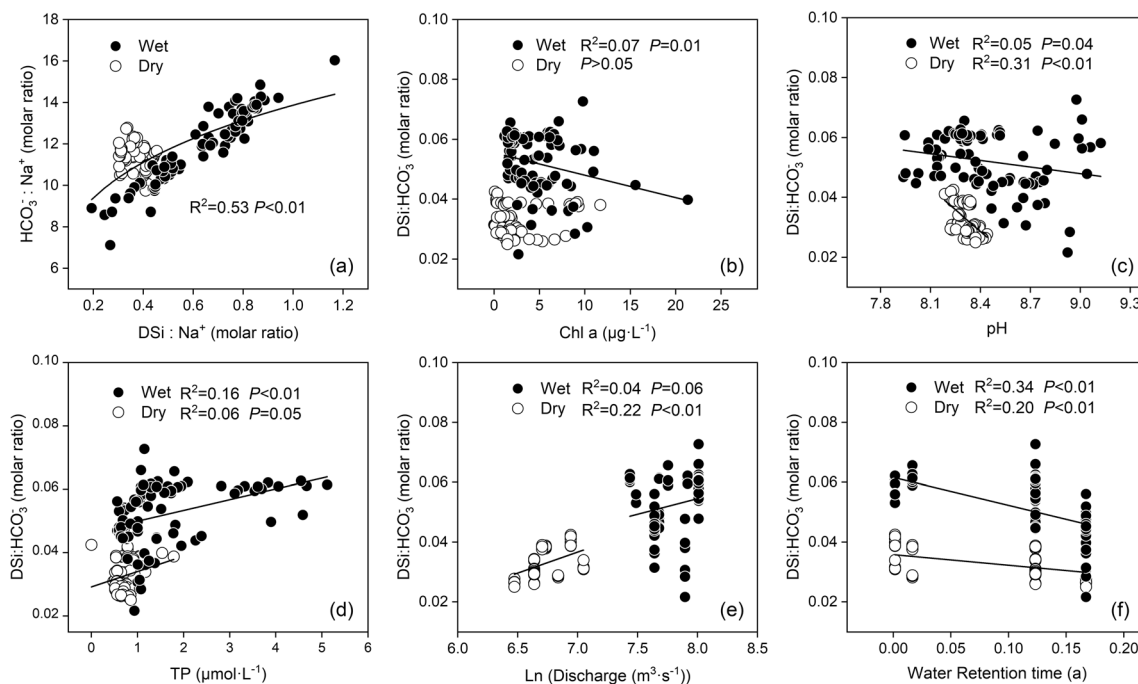


Fig. 5 Relationships between Na-normalized HCO₃⁻ and DSi (a), and between the DSi:HCO₃⁻ ratio and the environmental factors (b–f)

erosion processes and the dilution effect of HCO₃⁻ in the wet season. The DSi:HCO₃⁻ was significantly negatively correlated with the concentration of TDS in the wet season ($P < 0.01$), which was consistent with the results of the other watersheds (Wang et al. 2016; Li et al. 2018). The DSi:HCO₃⁻ ratio was significantly negatively correlated with water retention time (Fig. 5f). The reason was that the phytoplankton biomass greatly increased with water retention time, resulting in decreasing of the DSi:HCO₃⁻ ratio in the reservoirs (Fig. 3i, JP I and ET).

The DSi:HCO₃⁻ ratio was controlled by water retention time, discharge, and TP in the wet season (Eq. (7)). That is, in the wet season, the DSi:HCO₃⁻ ratio was influenced by the processes (including rainfall-runoff, rock weathering, and farming) outside the reservoir and in the reservoir process (aquatic organism growth). In the dry season, the DSi:HCO₃⁻ ratio was greatly influenced by TDS, pH, and Chl a concentration (formula (8)). The material/energy exchange between the reservoir system and its surrounding environment significantly decreased and resulted in the disappearance of thermal stratification and the stability of the water system. The coupling processes of the phytoplankton growth stoichiometrically assimilating DSi and HCO₃⁻ and the microbial decomposition forming HCO₃⁻ resulted in DSi:HCO₃⁻ ratio decreasing within the reservoir, i.e., the DSi:HCO₃⁻ ratio was mainly controlled by biological processes within the cascade reservoirs.

Retention of DSi and DIC in the cascade reservoirs

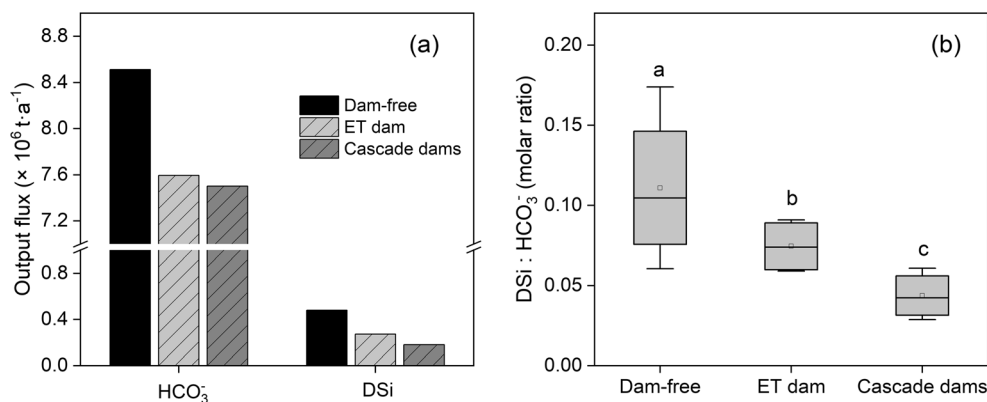
The water body retention time was prolonged from 45 to 126.6 days with cascade damming in the LYLJR (Fig. 1b),

and the mean monthly inflow (ranging from 16.67×10^8 to 139.13×10^8 m³) was closed to the mean monthly outflow (ranging from 24.18×10^8 to 99.34×10^8 m³) of the cascade reservoirs in the LYLJR (Fig. 2c), being consistent with the characteristics of the runoff reservoir, which to some extent to ensure the water demand ratio for the ecosystems in the hot-dry valley and phytoplankton growth in the reservoirs.

In terms of the primary production of phytoplankton, the DSi and HCO₃⁻ sequestered by phytoplankton in the cascade reservoirs was 3.46×10^4 t·Si a⁻¹ and 1.89×10^4 t·C a⁻¹, accounting for 15% of the DSi and 0.5% of the HCO₃⁻ of the inflow, respectively. It was suggested that a considerable amount of DSi and HCO₃⁻ in the form of organic matter were sequestered in the cascade reservoirs in the LYLJR. Consequently, the cascading dams could extend the biogeochemical coupling cycle of C and Si in inland aquatic ecosystems.

Dead phytoplankton, especially diatoms, sink faster than other algae, decomposed and/or deposited at the reservoir bottom (Maavara et al. 2014; Ran et al. 2016), increasing the DSi:HCO₃⁻ ratio at the deep/bottom of the reservoir water column (Fig. 4). The increase in diatom biomass and its deposition were considered to be the main process of DSi loss in the top layer of the reservoirs (Frings et al. 2014). The DSi:HCO₃⁻ ratio increased significantly ($P = 0.002$) from the upper JP I reservoir to the downstream of the TZL dam (Fig. 3i). This phenomenon was due to the higher DSi:HCO₃⁻ ratio in the released water (Y11, Y5, Y1 in Fig. 3i). On the basis of the operation scheme of the reservoirs, the released water through the dams was mainly from the deep/bottom reservoir

Fig. 6 Comparison of the output flux of HCO_3^- and DSi at the mouth of Yalongjiang River (a), the DSi: HCO_3^- ratio in the LYLJR mainstream in the case of dam-free, the ET dam only, and the cascade dams, respectively (b) (partial data from (Chen et al. 2002; Li et al. 2014)). Different letters indicate significant differences at $P < 0.05$

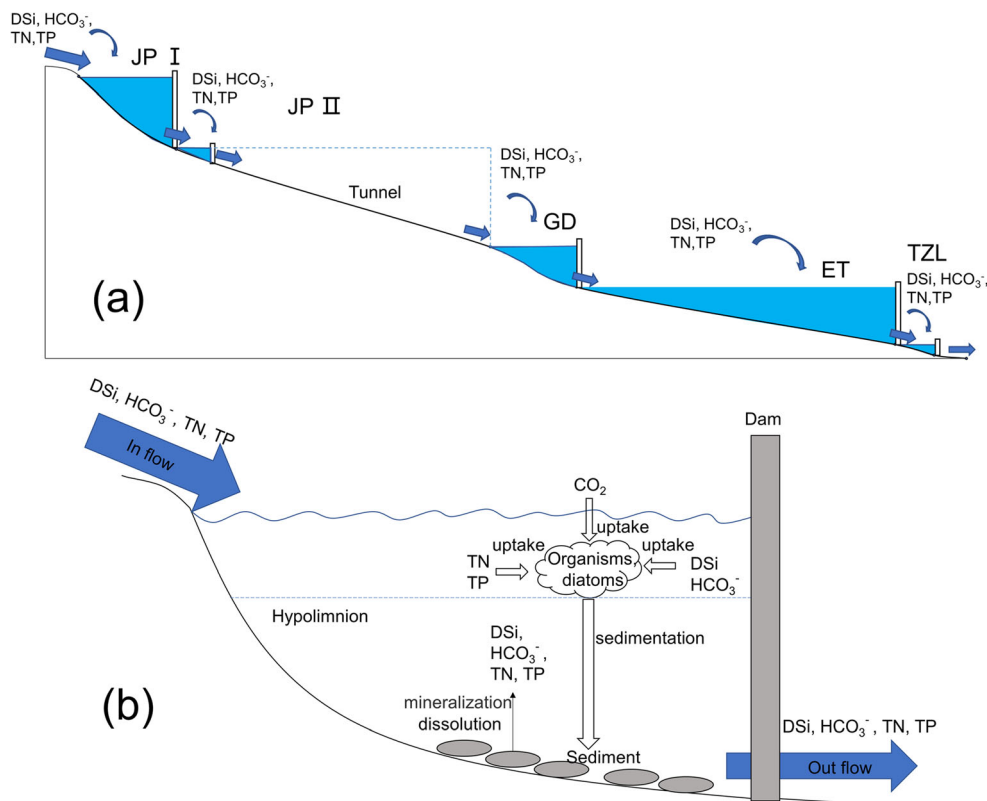


water body with higher ratio of DSi: HCO_3^- . Consequently, the ratio of DSi: HCO_3^- (0.044) was lower in the reservoir water than that (0.052) at the mouth of the Yalongjiang river. However, the DSi: HCO_3^- ratio (0.052) at the mouth of the Yalongjiang river was slightly lower than that (0.059) in the upper-middle reach of the Yalongjiang River (Li et al. 2014), which evidenced the retention of DSi in the operating cascade damming too.

At the mouth of Yalongjiang River, the export flux of HCO_3^- and DSi was $7.50 \times 10^6 \text{ t a}^{-1}$ (with error -6.97%) and $0.18 \times 10^6 \text{ t a}^{-1}$ (with error -1.15%), respectively, and the mean DSi: HCO_3^- ratio was 0.052 ± 0.008 with the cascade damming in the mainstream of the LYLJR (Fig. 6).

However, the export flux of HCO_3^- and DSi (the data from Chen et al. (2002)) was $8.51 \times 10^6 \text{ t a}^{-1}$ and $0.48 \times 10^6 \text{ t a}^{-1}$, respectively, the mean DSi: HCO_3^- ratio was (0.111 ± 0.024) in the case of dam-free in the mainstream of the LYLJR (Fig. 6). Clearly, the export flux of HCO_3^- and DSi as well as the DSi: HCO_3^- ratio decreased by the cascade damming in the mainstream of the LYLJR. Compared with the situation of dam-free in the LYLJR, the export flux of HCO_3^- and DSi at the mouth of the Yalongjiang River was reduced by 11.87% and 62.50%, respectively; the DSi: HCO_3^- ratio was reduced by 36.01% and 53.15% with the ET damming only and cascade damming in the mainstream of the LYLJR, respectively.

Fig. 7 a Conceptual model of the coupling carbon and silicon cycle in the cascade reservoirs. The straight arrow indicates the upstream input, and the curved arrow denotes the input from tributaries and reservoir surrounding, respectively. b The carbon and silicon cycle within the reservoirs



Migration and transformation of C and Si in reservoirs

Based on the above analysis, a conceptual model of DSi and C cycle with cascade damming in the LYLJR was established (Fig. 7).

It is assumed that the DSi and HCO_3^- undergo the same path (surface water body–phytoplankton–deep water body) from JP I to TZL reservoir. The DSi and HCO_3^- from the upstream or around the reservoir are transported into the water body of the cascade reservoirs in the LYLJR (Fig. 7a). In reservoirs, the biomass of the phytoplankton and microorganisms increases with the water flow slowing down and increasing water retention time. Both dissolved CO_2 and HCO_3^- serve as the inorganic carbon source (Tortell et al. 1997), while DSi is the only silicon source required for the phytoplankton, especially diatom growing. Consequently, phytoplankton photosynthesis caused the decrease of DSi and HCO_3^- in the surface waters (Beaulieu et al. 2010; Wang et al. 2016). The dead phytoplankton is then decomposed and/or deposited at the bottom of the water body (Maavara et al. 2014; Ran et al. 2016). The dissolution and mineralization of biogenic silica and organic carbon (OC) in sediments is limited by the environmental conditions (temperature, light, anoxic environment, etc.) (Loucaides et al. 2012; Isidorova et al. 2019). Compared to organic carbon, DSi has a higher recycling efficiency (Maavara et al. 2014, 2017), but more DSi is absorbed by phytoplankton and eventually trapped in the reservoir (Frings et al. 2014). Therefore, both the retention of DSi by phytoplankton and the conversion of OC to DIC by microorganisms cause the decrease of DSi: HCO_3^- in the water column (Fig. 7b). The average ratio of silicon to carbon (0.79) of freshwater diatoms (Sicko-Goad et al. 1984; Tortell et al. 1997) is much larger than that (0.048) in river water of the LYLJR. The phytoplankton biomass in the reservoirs of the JP I, GD, ET, and TZL was higher than that of the watercourse in the LYLJR. A considerable amount of DSi and DIC were sequestered in the cascade reservoirs. Consequently, the cascading dams could extend the biogeochemical coupling cycle of C and Si in inland aquatic ecosystems.

Conclusion

River cascade damming may alter the biogeochemical cycle of the riverine DIC and DSi by increasing biological processes in reservoirs. The lower ratio of DSi to HCO_3^- (0.044 ± 0.001) was mainly controlled by the domination of carbonate mineral in the sedimentary rock of the Yalongjiang River drainage basin. The DSi: HCO_3^- ratio was positively correlated with discharge ($P < 0.05$), and negatively correlated with the water retention time ($P < 0.01$) and Chl a, implying that the variations of DSi: HCO_3^- ratio were mainly determined by the rock

chemical weathering processes and the hydrologic process outside the reservoirs and the biological processes within the cascade reservoirs. The phytoplankton photosynthetic process stoichiometrically assimilated DSi and HCO_3^- , resulted in $3.46 \times 10^4 \text{ t-Si a}^{-1}$ and $1.89 \times 10^4 \text{ t-C a}^{-1}$ sequestering in the cascade reservoirs, respectively. Compared with the situation of dam-free in the LYLJR, the export flux of HCO_3^- and DSi at the mouth of Yalongjiang River was reduced by 11.87% and 62.50%, respectively; the ratio of DSi: HCO_3^- decreased by 36.01% for only building the ET dam and 53.15% for the cascade damming, respectively. The water renewal time prolonged from 45 to 126.6 days due to the regulation of the cascade reservoirs in the mainstream. Ultimately, a conceptual model on migration-transformation of DIC and DSi in the cascade reservoirs in the LYLJR was established. These findings demonstrated that riverine cascade damming could extend the biogeochemical coupling cycle of DIC and DSi within the inland aquatic ecosystems and ensure the ecological environment security in the hot-dry valley.

Acknowledgments We are grateful to Cui Xiaoyang, Zheng Xiangyu, and Zhang Runkai for their help in the fieldwork; and the editor and two anonymous reviewers for their constructive reviews.

Funding information This study was supported by the National Natural Science Foundation of China (Grant No. 41771216 and No. 41871014).

References

- Amiotte Suchet P, Probst JL (1993) Modelling of atmospheric CO_2 consumption by chemical weathering of rocks: application to the Garonne, Congo and Amazon basins. *Chem Geol* 107:205–210. [https://doi.org/10.1016/0009-2541\(93\)90174-H](https://doi.org/10.1016/0009-2541(93)90174-H)
- APHA (2005) Standard methods for the examination of water and wastewater. Am Public Heal Assoc Washington, DC, USA
- Assmy P, Smetacek V, Montresor M, Klaas C, Henjes J, Strass VH, Arrieta JM, Bathmann U, Berg GM, Breitbarth E, Cisewski B, Friedrichs L, Fuchs N, Herndl GJ, Jansen S, Kragefsky S, Latasa M, Peeken I, Rottgers R, Scharek R, Schuller SE, Steigenberger S, Webb A, Wolf-Gladrow D (2013) Thick-shelled, grazer-protected diatoms decouple ocean carbon and silicon cycles in the iron-limited Antarctic circumpolar current. *Proc Natl Acad Sci* 110:20633–20638. <https://doi.org/10.1073/pnas.1309345110>
- Beaulieu E, Godd eris Y, Labat D, Roelandt C, Oliva P, Guerrero B (2010) Impact of atmospheric CO_2 levels on continental silicate weathering. *Geochemistry, Geophys Geosystems* 11. <https://doi.org/10.1029/2010GC003078>
- Behrenfeld MJ, Falkowski PG (1997) Photosynthetic rates derived from satellite-based chlorophyll concentration. *Limnol Oceanogr* 42:1–20. <https://doi.org/10.4319/lo.1997.42.1.0001>
- Brzezinski MA (1985) The Si:C:N ratio of marine diatoms: interspecific variability and the effect of some environmental variables. *J Phycol* 21:347–357
- Cad ee GC, Hegeman J (1974) Primary production of phytoplankton in the Dutch Wadden Sea. *Netherlands J, Sea Res*
- Carey JC, Fulweiler RW (2012) Human activities directly alter watershed dissolved silica fluxes. *Biogeochemistry* 111:125–138. <https://doi.org/10.1007/s10533-011-9671-2>

- Castello L, Macedo MN (2016) Large-scale degradation of Amazonian freshwater ecosystems. *Glob Chang Biol* 22:990–1007. <https://doi.org/10.1111/gcb.13173>
- Chen J, Wang F, Xia X, Zhang L (2002) Major element chemistry of the Changjiang (Yangtze River). *Chem Geol* 187:231–255. [https://doi.org/10.1016/S0009-2541\(02\)00032-3](https://doi.org/10.1016/S0009-2541(02)00032-3)
- Clark I, Fritz P (1997) Environmental isotopes in hydrogeology. CRC Press/Lewis Publishers
- Conley DJ (2002) Terrestrial ecosystems and the global biogeochemical silica cycle. *Glob Biogeochem Cycles* 16:68–1–68–8. <https://doi.org/10.1029/2002GB001894>
- Cui G, Li X, Li Q, Huang J, Tao Y, Li S, Zhang J (2017) Damming effects on dissolved inorganic carbon in different kinds of reservoirs in Jialing River, Southwest China. *Acta Geochim* 36:581–597. <https://doi.org/10.1007/s11631-017-0155-5>
- Das A, Krishnaswami S, Bhattacharya SK (2005) Carbon isotope ratio of dissolved inorganic carbon (DIC) in rivers draining the Deccan traps, India: sources of DIC and their magnitudes. *Earth Planet Sci Lett* 236:419–429. <https://doi.org/10.1016/j.epsl.2005.05.009>
- Fang F, Hong Z, Zhe L et al (2010) Spatio-temporal variations of euphotic depth and its causing factors in Xiaojiang River backwater area of three gorges. *Adv Water Sci* 21:113–119
- Frings PJ, Clymans W, Jeppesen E, Lauridsen TL, Struyf E, Conley DJ (2014) Lack of steady-state in the global biogeochemical Si cycle: emerging evidence from lake Si sequestration. *Biogeochemistry* 117:255–277. <https://doi.org/10.1007/s10533-013-9944-z>
- Gaillardet J, Dupré B, Louvat P, Allègre CJ (1999) Global silicate weathering and CO₂ consumption rates deduced from the chemistry of large rivers. *Chem Geol* 159:3–30. [https://doi.org/10.1016/S0009-2541\(99\)00031-5](https://doi.org/10.1016/S0009-2541(99)00031-5)
- Gao Q, Tao Z, Huang X, Nan L, Yu K, Wang Z (2009) Chemical weathering and CO₂ consumption in the Xijiang River basin, South China. *Geomorphology* 106:324–332. <https://doi.org/10.1016/j.geomorph.2008.11.010>
- Guildford SJ, Hecky RE (2000) Total nitrogen, total phosphorus, and nutrient limitation in lakes and oceans: is there a common relationship? *Limnol Oceanogr* 45:1213–1223. <https://doi.org/10.4319/lo.2000.45.6.1213>
- He Z, Zhang X, Bao S, Qiao Y, Sheng Y, Liu X, He X, Yang X, Zhao J, Liu R, Lu C (2015) Multiple climatic cycles imprinted on regional uplift-controlled fluvial terraces in the lower Yalong River and Anning River, SE Tibetan plateau. *Geomorphology* 250:95–112. <https://doi.org/10.1016/j.geomorph.2015.08.010>
- Hélie JF, Hillaire-Marcel C, Rondeau B (2002) Seasonal changes in the sources and fluxes of dissolved inorganic carbon through the St. Lawrence River - isotopic and chemical constraint. *Chem Geol* 186:117–138. [https://doi.org/10.1016/S0009-2541\(01\)00417-X](https://doi.org/10.1016/S0009-2541(01)00417-X)
- Hughes HJ, Bouillon S, André L, Cardinal D (2012) The effects of weathering variability and anthropogenic pressures upon silicon cycling in an intertropical watershed (Tana River, Kenya). *Chem Geol* 308–309:18–25. <https://doi.org/10.1016/j.chemgeo.2012.03.016>
- Isidorova A, Mendonça R, Sobek S (2019) Reduced mineralization of terrestrial OC in anoxic sediment suggests enhanced burial efficiency in reservoirs compared to other depositional environments. *J Geophys Res Biogeosci* 124:678–688. <https://doi.org/10.1029/2018JG004823>
- Jiu Y, Yu B, Li Z et al (2018) Variation trend and correlation analysis of water quality in recent 5 years in Ertan reservoir. *Sichuan Environ* 37:88–94. <https://doi.org/10.14034/j.cnki.schj.2018.06.014>
- Kolasa-Wiecek A (2015) Stepwise multiple regression method of greenhouse gas emission modeling in the energy sector in Poland. *J Environ Sci (China)* 30:47–54. <https://doi.org/10.1016/j.jes.2014.09.037>
- Li SL, Chetelat B, Yue F, Zhao Z, Liu CQ (2014) Chemical weathering processes in the Yalong River draining the eastern Tibetan plateau, China. *J Asian Earth Sci* 88:74–84. <https://doi.org/10.1016/j.jseas.2014.03.011>
- Li S, Chen Y, Zhang Q (2017) 11-year change in water chemistry of large freshwater reservoir Danjiangkou, China. *J Hydrol* 551:508–517. <https://doi.org/10.1016/j.jhydrol.2017.05.058>
- Li T, Li S, Bush RT, Liang C (2018) Extreme drought decouples silicon and carbon geochemical linkages in lakes. *Sci Total Environ* 634:1184–1191. <https://doi.org/10.1016/j.scitotenv.2018.04.074>
- Loucaides S, Van Cappellen P, Roubeix V et al (2012) Controls on the recycling and preservation of biogenic silica from biomineralization to burial. *Silicon* 4:7–22. <https://doi.org/10.1007/s12633-011-9092-9>
- Lu T, Chen N, Duan S, Chen Z, Huang B (2016) Hydrological controls on cascade reservoirs regulating phosphorus retention and downriver fluxes. *Environ Sci Pollut Res* 23:24166–24177. <https://doi.org/10.1007/s11356-016-7397-3>
- Maavara T, Dürr HH, Van Cappellen P (2014) Worldwide retention of nutrient silicon by river damming: from sparse data set to global estimate. *Glob Biogeochem Cycles* 28:842–855. <https://doi.org/10.1002/2014GB004875>
- Maavara T, Lauerwald R, Regnier P, Van Cappellen P (2017) Global perturbation of organic carbon cycling by river damming. *Nat Commun* 8:15347. <https://doi.org/10.1038/ncomms15347>
- Macuiane MA, Kaunda EKW, Jamu D (2011) Seasonal dynamics of physico-chemical characteristics and biological responses of Lake Chilwa, southern Africa. *J Great Lakes Res* 37:75–82. <https://doi.org/10.1016/j.jglr.2010.12.009>
- Meybeck M (1987) Global chemical weathering of surficial rocks estimated from river dissolved loads. *Am J Sci* 287:401–428. <https://doi.org/10.2475/ajs.287.5.401>
- Mosley LM, Zammit B, Leyden E, Heneker TM, Hipsey MR, Skinner D, Aldridge KT (2012) The impact of extreme low flows on the water quality of the lower Murray River and lakes (South Australia). *Water Resour Manag* 26:3923–3946. <https://doi.org/10.1007/s11269-012-0113-2>
- Olds BP, Peterson BC, Koupal KD, Farnsworth-Hoback KM, Schoenebeck CW, Hoback WW (2011) Water quality parameters of a Nebraska reservoir differ between drought and normal conditions. *Lake Reserv Manag* 27:229–234. <https://doi.org/10.1080/07438141.2011.601401>
- Parr JF, Sullivan LA (2011) Phytolith occluded carbon and silica variability in wheat cultivars. *Plant Soil* 342:165–171. <https://doi.org/10.1007/s11104-010-0680-z>
- Peng X, Congqiang L, Wang B, Yanchuang Z (2014) The impact of damming on geochemical behavior of dissolved inorganic carbon in a karst river. *Chin Sci Bull* 59:366–373. <https://doi.org/10.1007/s11434-014-0153-5>
- Powers SM, Tank JL, Robertson DM (2015) Control of nitrogen and phosphorus transport by reservoirs in agricultural landscapes. *Biogeochemistry* 124:417–439. <https://doi.org/10.1007/s10533-015-0106-3>
- Ran X, Yu Z, Yao Q, Chen H, Guo H (2013) Silica retention in the three gorges reservoir. *Biogeochemistry* 112:209–228. <https://doi.org/10.1007/s10533-012-9717-0>
- Ran X, Liu S, Liu J, Zang J, Che H, Ma Y, Wang Y (2016) Composition and variability in the export of biogenic silica in the Changjiang River and the effect of three gorges reservoir. *Sci Total Environ* 571:1191–1199. <https://doi.org/10.1016/j.scitotenv.2016.07.125>
- Schindler DW, Hecky RE, Findlay DL, Stainton MP, Parker BR, Paterson MJ, Beaty KG, Lyng M, Kasian SEM (2008) Eutrophication of lakes cannot be controlled by reducing nitrogen input: results of a 37-year whole-ecosystem experiment. *Proc Natl Acad Sci* 105:11254–11258. <https://doi.org/10.1073/pnas.0805108105>
- Sicko-Goad LM, Schelske CL, Stoermer EF (1984) Estimation of intracellular carbon and silica content of diatoms from natural

- assemblages using morphometric techniques. *Limnol Oceanogr* 29: 1170–1178. <https://doi.org/10.4319/lo.1984.29.6.1170>
- Song Z, Liu H, Strömberg CAE, Yang X, Zhang X (2017) Phytolith carbon sequestration in global terrestrial biomes. *Sci Total Environ* 603–604:502–509. <https://doi.org/10.1016/j.scitotenv.2017.06.107>
- Sterner R., Elser J. (2002) Ecological stoichiometry: the biology of elements from molecules to the biosphere: Robert W. Sterner, James J. Elser, Peter Vitousek: 9780691074917: [Amazon.com](https://www.amazon.com): books
- Syvitski JPM, Vörösmarty CJ, Kettner AJ, Green P (2005) Impact of humans on the flux of terrestrial sediment to the global coastal ocean. *Science* (80-) 308:376–380. <https://doi.org/10.1126/science.1109454>
- Taylor LL, Quirk J, Thorley RMS, Kharecha PA, Hansen J, Ridgwell A, Lomas MR, Banwart SA, Beerling DJ (2016) Enhanced weathering strategies for stabilizing climate and averting ocean acidification. *Nat Clim Chang* 6:402–408. <https://doi.org/10.1038/nclimate2882>
- The Editorial Committee for Vegetation Map of China (2001) Vegetation atlas of China. Science Press, Beijing
- Tortell PD, Reinfelder JR, Morel FMM (1997) Active uptake of bicarbonate by diatoms. *Nature* 390:243–244. <https://doi.org/10.1038/36765>
- Tréguer PJ, De La Rocha CL (2013) The World Ocean silica cycle. *Annu Rev Mar Sci* 5:477–501. <https://doi.org/10.1146/annurev-marine-121211-172346>
- Triplett LD, Engstrom DR, Conley DJ (2012) Changes in amorphous silica sequestration with eutrophication of riverine impoundments. *Biogeochemistry* 108:413–427. <https://doi.org/10.1007/s10533-011-9608-9>
- Wang B, Liu CQ, Wang F, Chetelat B, Maberly SC (2013) Diatoms modify the relationship between dissolved silicon and bicarbonate in impounded rivers. *J Limnol* 72:494–504. <https://doi.org/10.4081/jlimnol.2013.e40>
- Wang B, Liu CQ, Wang F, Liu XL, Wang ZL (2015) A decrease in pH downstream from the hydroelectric dam in relation to the carbon biogeochemical cycle. *Environ Earth Sci* 73:5299–5306. <https://doi.org/10.1007/s12665-014-3779-3>
- Wang B, Liu CQ, Maberly SC, Wang F, Hartmann J (2016) Coupling of carbon and silicon geochemical cycles in rivers and lakes. *Sci Rep* 6: 1–6. <https://doi.org/10.1038/srep35832>
- Wen Z, Song K, Shang Y, Fang C, Li L, Lv L, Lv X, Chen L (2017) Carbon dioxide emissions from lakes and reservoirs of China: a regional estimate based on the calculated pCO₂. *Atmos Environ* 170:71–81. <https://doi.org/10.1016/j.atmosenv.2017.09.032>
- Winemiller KO, McIntyre PB, Castello L et al (2016) Balancing hydro-power and biodiversity in the Amazon, Congo, and Mekong. *Science* (80-) 351:128–129. <https://doi.org/10.1126/science.aac7082>
- Wu NC, Tang T, Li DF et al (2009) Benthic algal communities in Jinping reach of Yalong River and its main tributaries in relation to environmental variables. *Acta Ecol Sin* 29:1697–1703
- Wu N, Sudebilige GJ et al (2010) Evaluation of an ecosystem service for avoiding phosphorus nonpoint source pollution of aquatic environment and its economic value: a case study from Ertan reservoir in Yalong River. *Acta Ecol Sin* 30:1734–1743
- Yan Z, Han W, Peñuelas J, Sardans J, Elser JJ, du E, Reich PB, Fang J (2016) Phosphorus accumulates faster than nitrogen globally in freshwater ecosystems under anthropogenic impacts. *Ecol Lett* 19: 1237–1246. <https://doi.org/10.1111/ele.12658>
- Zhang L, Qin X, Liu P, Huang Q (2016a) Chemical denudation rate and atmospheric CO₂ consumption by H₂CO₃ and H₂SO₄ in the Yangtze River catchment. *Acta Geol Sin* 90:1933–1943
- Zhang Q, Tao Z, Ma Z et al (2016b) Riverine hydrochemistry and CO₂ consumption in the tropic monsoon region: a case study in a granite-hosted basin, Hainan Island, China. *Environ Earth Sci* 75. <https://doi.org/10.1007/s12665-016-5250-0>

Publisher's note Springer Nature remains neutral with regard to jurisdictional claims in published maps and institutional affiliations.